Northward movement of the 30–50 day mode in an axisymmetric global spectral model

R. Krishnan, S. V. Kasture and R. N. Keshavamurty
Theoretical Physics Division, Physical Research Laboratory, Ahmedabad 380 009, India

We have used an axisymmetric version of a 5-level nonlinear global spectral model to study the meridional propagation of convective zones, with an aim to understand the movement of the equatorial 30–50 day mode in the Indian monsoon region. The monsoonal type of circulation is caused due to the north–south differential heating in the Indian subcontinent. We have modelled the evolution of perturbations superposed on this basic flow. When cumulus heating (CISK) is included it is found that the cloud zones migrate northward. Our calculations show that the northward speed is about 0.5° per day.

THE large thermal contrast in the meridional direction sets up the monsoonal circulation in the Indian subcontinent. The purpose of this study is to model the northward propagation of convective activity in the Indian monsoon region to understand the relation between the equatorial 30–50 day oscillation and the variability of the Indian summer monsoon. We now briefly mention some salient features of this oscillation relevant to this study. Observations suggest that the east–west-oriented cloud bands appear quite prominently between 70°E and 95°E and extend up to 600 mb pressure level in the vertical. Observations also reveal that these cloud zones penetrate from the equatorial regions to about 30°N in the Indian monsoon region with a speed of around 1° latitude per day. The study will be of relevance in the understanding of active and break phases of monsoons.

There are studies that relate the low-frequency fluctuations of monsoon activity with the well known 30–50 day oscillation found by Madden and Julian[1]. Krishnamurti and Subrahmanyam[2], Krishnamurti *et al.*[3], and Murakami and Nakazawa[4] found the northward propagation of the 30–50 day mode over India during MONEX with a meridional speed of roughly 1° per day by the diagnostic studies on FGGE data. Similarly Sikka and Gadgil[5] found from satellite observations that cloud patches propagate northward in the Indian monsoon region on the time scale of the equatorial intraseasonal oscillation. Knutson *et al.*[6] and Lau and Chan[7] on the basis of OLR data for several northern summers identified migrating convective zones in the Indian monsoon region. Yasunari[8,9] reported the meridional movement of convective activity and its association with the active–break monsoon cycles using satellite pictures of cloudiness of South Asia.

Lau and Lau[10] have analysed the intraseasonal oscillations appearing in the 12-year duration of a GCM experiment performed at the Geophysical Fluid Dynamics Laboratory (GFDL). They have studied the connection between the oscillatory behaviour in the tropics and the monsoon activity over South Asia in summer. Kasture and Keshavamurty[11] did a power spectrum analysis of the zonal wind and found a large power occurred on time scales of 30–50 days. Webster and Chou[12] used a zonally symmetric moist primitive equation model coupled to an interactive ocean to study the low-frequency intraseasonal transients of the monsoon system. They showed that the low-frequency variations were the result of feedbacks between the hydrologic cycle and the differential heating between the interactive ocean and continental areas. Webster[13] and Goswami and Shukla[14] included physical processes like moist convection and surface hydrology feedback to simulate the northward movement of the wave disturbances in the monsoon region. Keshavamurty *et al.*[15] calculated the 'meridional refractive index' of this mode and showed that it propagates in the meridional direction. Keshavamurty *et al.*[16] obtained a rough estimate of the northward phase speed of this mode to be around a few ms^{-1}.

We have used an axisymmetric version of a 5-level nonlinear global spectral model for our present study. We have studied the impact of cumulus heating (CISK) on the perturbations superposed on a generated monsoon type of basic flow. Charney and Eliassen[17] proposed the CISK mechanism to explain the development of tropical depressions. They showed that in a conditionally unstable atmosphere the interaction between the large-scale motion and the small-scale cumulus convection works in such a way that the latent heat due to cumulus scale convection is derived from the large-scale frictional convergence of moisture. The small-scale cumulus clouds thus supply latent heat energy to the cyclone and the cyclone supports the cumulus cell by producing low-level convergence of moisture.

Gadgil[18] showed that the variability of the ITCZ activity arises out of a nonlinear interaction between the small-scale cumulus clouds and the synoptic scale

motion. We have used the CISK mechanism to study *the northward propagation of the convective bands in* the Indian summer monsoon region.

The model

We have used an axisymmetric version of the 5-level nonlinear global spectral model described in Bourke[19], for our present study. The symmetric equations are obtained by setting $\frac{\partial}{\partial\lambda}=0$. The vertical σ levels are shown in Figure 1. The prognostic and diagnostic equations are given below:

$$\frac{\partial\zeta}{\partial t}=-\frac{1}{a\cos\phi}\frac{\partial B}{\partial\phi}-2\Omega\left(\sin\phi D+\frac{V}{a}\right)+K_h\left[\frac{1}{a^2}\frac{\partial^2\zeta}{\partial\phi^2}+2\frac{\zeta}{a^2}\right]-\varepsilon\zeta \quad (1)$$

$$\frac{\partial D}{\partial t}=-\frac{1}{a\cos\phi}\frac{\partial A}{\partial\phi}+2\Omega\left(\sin\phi\zeta-\frac{U}{a}\right)-\frac{1}{a^2}\frac{\partial^2}{\partial\phi^2}(E+\Phi'+RT_0q)+K_h\left[\frac{1}{a^2}\frac{\partial^2 D}{\partial\phi^2}+2\frac{D}{a^2}\right]-\varepsilon D \quad (2)$$

$$\frac{\partial q}{\partial t}=\frac{\bar V}{a}\frac{\partial q}{\partial\phi}+\bar D \quad (3)$$

$$\frac{\partial T}{\partial t}=-\frac{1}{a\cos\phi}\frac{\partial(VT')}{\partial\phi}+T'D+\dot\sigma\gamma+\frac{RT}{c_p}\left[\bar D+(V+\bar V)\frac{1}{a}\frac{\partial q}{\partial\phi}\right]+\frac{H_c}{c_p}+\frac{K_h}{a^2}\frac{\partial^2 T}{\partial\phi^2}-\delta T \quad (4)$$

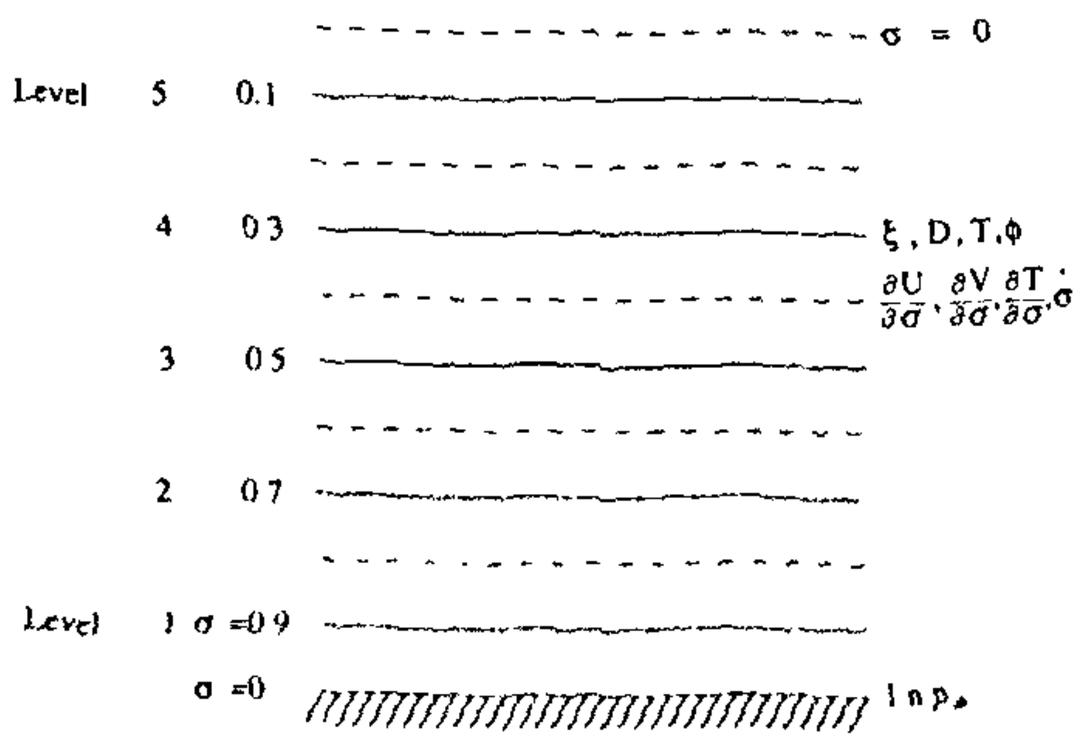

Figure 1. The vertical levels of the axisymmetric global spectral model

The diagnostic equation for vertical velocity $\dot\sigma$ is

$$\dot\sigma=[(1-\sigma)\bar D-\bar D^\sigma]+[(1-\sigma)\bar V-\bar V^\sigma]\frac{1}{a}\frac{\partial q}{\partial\phi}. \quad (5)$$

The terms in the above equations are explained below: a is the radius of the earth, ϕ the latitude, p_* the surface pressure, $\sigma=(p/p_*)$ the vertical coordinate, Ω the earth's rotation rate, R the gas constant, c_p the specific heat at constant pressure, $\gamma=\frac{RT}{\sigma c_p}-\frac{\partial T}{\partial\sigma}$ the static stability, H_c the prescribed rate of heating, ε the Rayleigh friction, δ the Newtonian cooling and K_h the horizontal diffusion coefficient, u the zonal velocity, v the meridional velocity; $U=u\cos\phi$, $V=v\cos\phi$, ζ the vertical component of relative vorticity, D the horizontal divergence, q log p_*, T the absolute temperature, Φ the geopotential height, $\dot\sigma$ the total time derivative of σ. A subscript zero denotes a horizontal mean value and the superscript prime the deviation from the mean.

$$A=\zeta U+\dot\sigma\frac{\partial V}{\partial\sigma}+\frac{RT'}{a}\cos\phi\frac{\partial q}{\partial\phi}$$

$$B=\zeta V-\dot\sigma\frac{\partial U}{\partial\sigma}$$

$$E=\frac{U^2+V^2}{2\cos^2\phi} \quad (6)$$

$$(\bar{\ })^\sigma=\int_1^\sigma(\ )\,\partial\sigma$$

$$(\bar{\ })=\int_1^0(\ )\,\partial\sigma\,.$$

The boundary conditions are $\dot\sigma=0$ at $\sigma=1$ and $\sigma=0$. The prognostic and diagnostic variables at each vertical level are expanded in terms of legendre polynomials in the meridional direction. For instance, the stream function ψ at a given model level is expanded as

$$\psi=\sum_{l=0}^{l=LMAX}\psi_l(l)\,P_l(\sin\phi).$$

The series was truncated at LMAX = 30. The nonlinear *advection terms are first calculated at grid points* and later on transformed into the wave number domain. The model equations are integrated using semi implicit time integration scheme. A time-step of 24 min was used in the model and the horizontal diffusion has been parametrized following Bourke *et al.*[20]. The horizontal diffusion coefficient K_h is chosen to be 6.25×10^4 $m^2\,s^{-1}$. The mean hemispheric temperatures at the different model levels are as follows: $T0_{standard}=277.5$ K,

$T0_{100mb} = 268.0$ K, $T0_{500mb} = 250.7$ K, $T0_{300mb} = 226.5$ K and $T0_{100mb} = 203.0$ K.

Results of numerical integration

First we generate monsoonal type of circulation using an appropriate heating distribution. A Rayleigh friction and Newtonian cooling of 5 days dissipation time scale have been used. The initial condition corresponds to an atmosphere at rest. The initial temperatures at the different model levels correspond to their respective mean hemispheric values already mentioned. The model equations have been integrated for 25 days after switching on the heat source. The forcing is kept fixed throughout the time of integration to attain a steady state. The steady-state zonal velocity distribution is shown in Figure 2. The low-level westerly flow and the upper level easterlies resemble the structure of the monsoonal basic flow pattern. The maximum westerly flow is at 700 mb and the maximum easterlies at 100 mb.

We now switch on an idealized equatorial heat source extending between 5° S and 5° N and integrate the model for five days. Now the equatorial heat source is turned off and cumulus heating (CISK) is imposed. We now examine the evolution of perturbations superposed on the background flow. The rate of non-adiabatic cumulus heating (CISK) is proportional to the relative vorticity at 900 mb (ζ_{900}) and is given by

$$\frac{\dot{Q}}{C_p} = H_f(p)\frac{p}{R} S\rho g \sqrt{\frac{K_e}{2f_0}} \sin(2\alpha_s)\zeta_{900}, \qquad (7)$$

where $\rho = 1.225\ kg^{-3}$ is the density of air, $K_e = 10\ m^2\ s^{-1}$ is the eddy viscosity coefficient, $a_s = 22.5°$ is the angle between the surface geostrophic wind and the surface isobars, $g = 9.81\ ms^{-2}$ is the acceleration due to gravity, S is the static stability parameter; f_0 is the coriolis parameter at 10° N, $H_f(p)$ is the function $\frac{\pi}{2} \sin(\pi\sigma)$ which is used to distribute the heating in the vertical. This function has a maximum value at 500 mb and is zero at the surface and top of the atmosphere. The value of S at 900 mb is $1.29 \times 10^{-6}\ m^2\ s^{-2}\ Pa^{-2}$.

Under the influence of CISK, the perturbations start growing. Figure 3 shows the meridional evolution of zonal velocity at 700 mb and Figure 1 shows the meridional evolution of relative vorticity at 700 mb from day 31 to day 55. Figure 5 shows the relative vorticity at 900 mb from day 31 to day 55. The distinct eastward tilt of the contours seen in the latitude–time cross-sections of Figures 3, 4 and 5 clearly suggests a northward movement of the disturbances. From Figures 4 and 5 it is seen that the cyclonic vortices advance northward with time, implying the meridional propagation of the convective zone. The northward propagation speed is about 0.5° per day which can be calculated roughly from the slope of the tilt. Our results

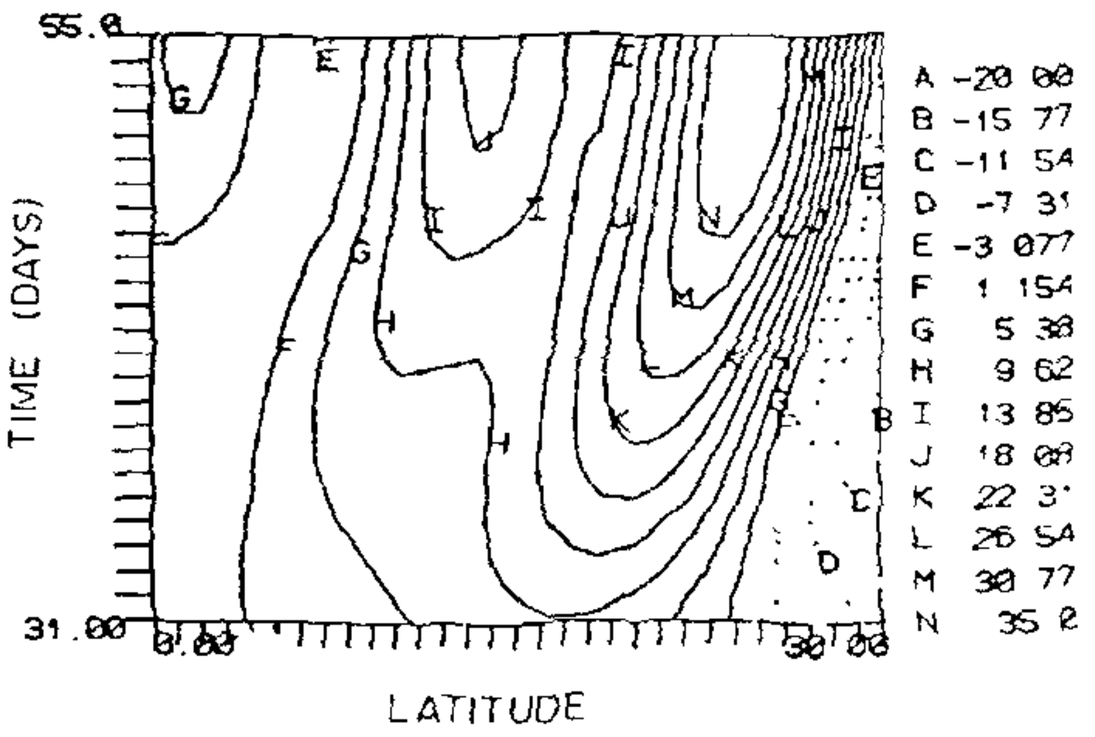

Figure 3. Latitude–time cross-section of zonal velocity (ms^{-1}) at 700 mb.

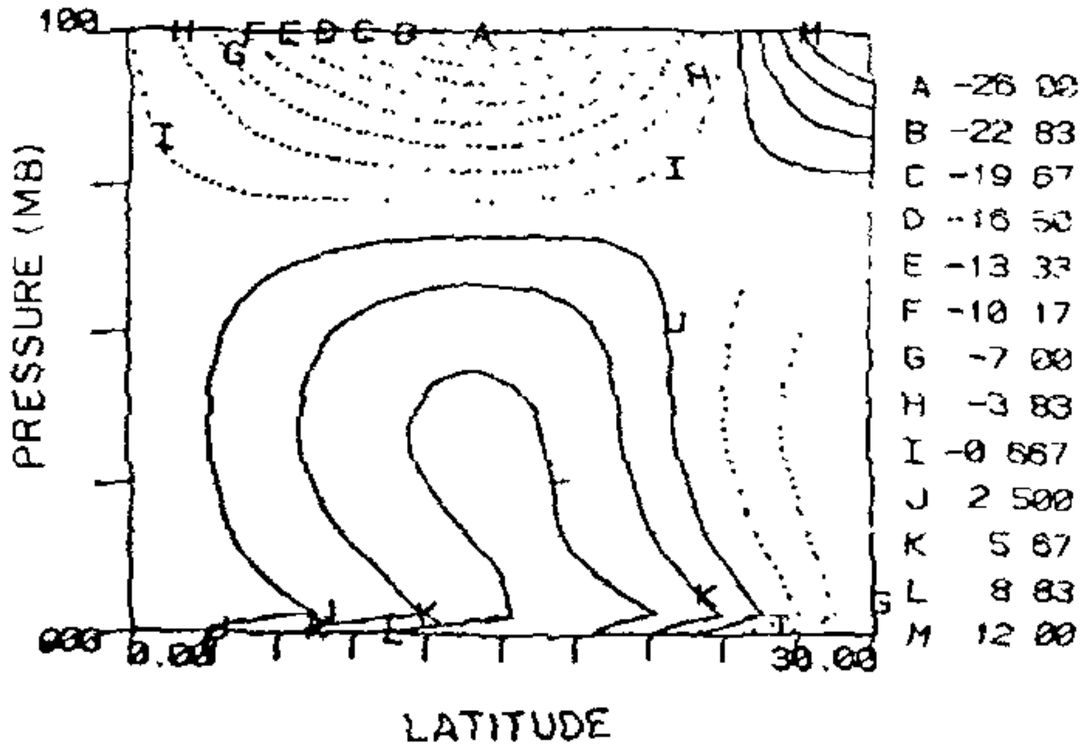

Figure 2. Model generated basic flow. Latitude pressure cross-section of zonal velocity (ms^{-1}).

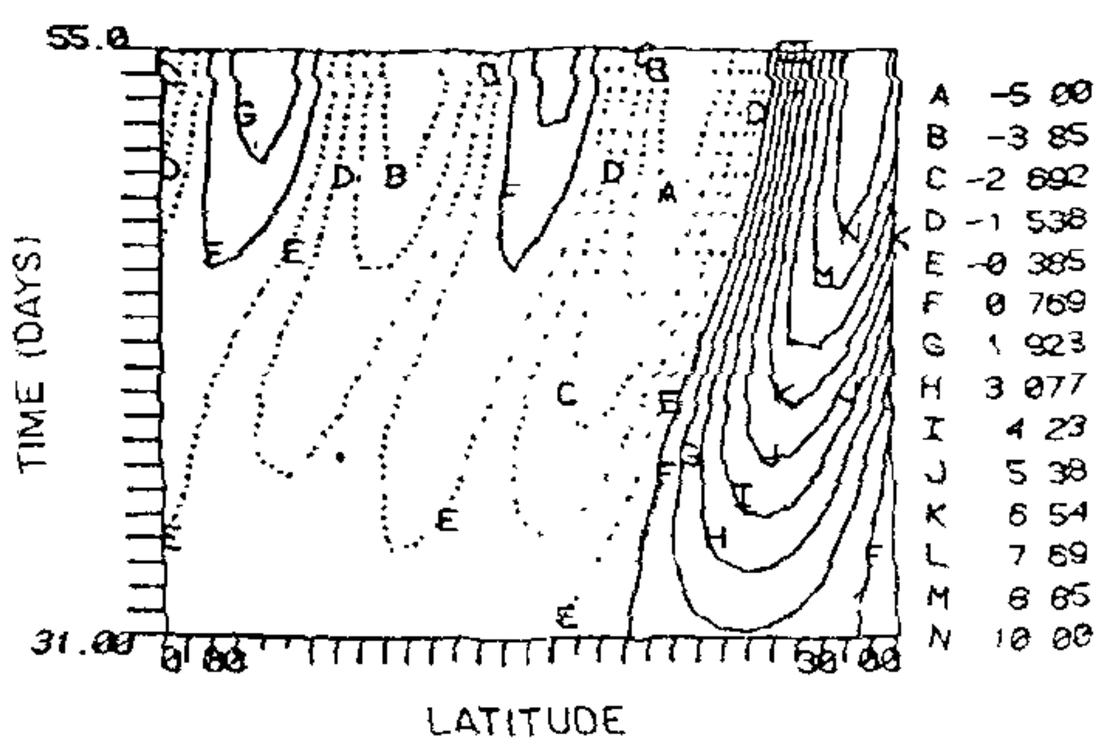

Figure 4. Latitude–time cross-section of relative vorticity ($10^{-5}s^{-1}$) at 700 mb.

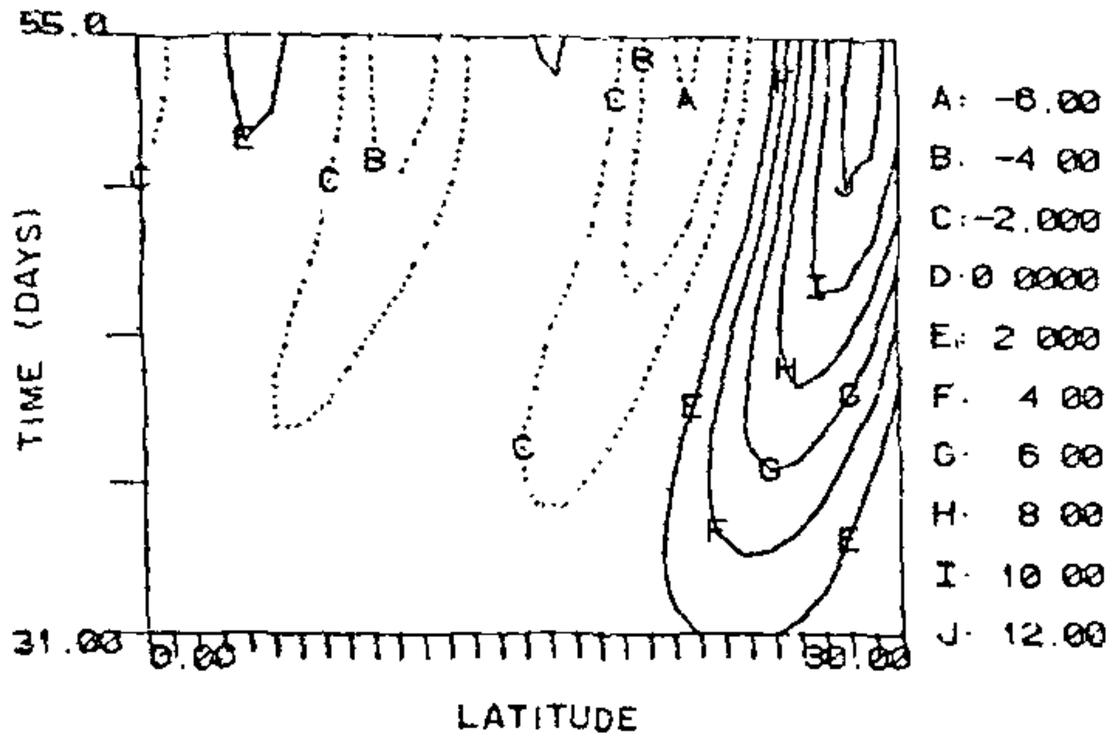

Figure 5. Latitude–time cross-section of relative vorticity ($10^{-5}s^{-1}$) at 900 mb.

also indicate that the northward penetration of the convective activity is mostly in the lower and middle troposphere. There is no meridional propagation above the 500 mb pressure level. This result is in conformity with the observations of Kasture and Keshavamurty[11]. Our results do not show any northward propagation of the perturbations beyond 32° N even at the lower levels.

The physical basis for the northward movement that we obtain in our numerical experiment is due to the presence of a strong north–south heating gradient which sets up a Hadley circulation. The basic zonal wind has a shear in the meridional direction. On imposing Charney's CISK (which assumes that cumulus heating is proportional to the low-level relative vorticity) a northward penetration of the perturbations is obtained. This is because of the meridional phase difference between the heating distribution and the zonal wind.

Conclusions

We have modelled the northward migration of the convective zones in the Indian summer monsoon region using an axisymmetric 5-level nonlinear global spectral model. We carried out this study to understand the meridional propagation of the 30–50 day mode in the Indian longitudes during the Northern hemispheric summer. A monsoon type of basic flow is generated in the model. An equatorial heating is temporarily switched on to generate perturbations near the equatorial region. In the presence of cumulus heating (CISK) a northward propagation of the disturbances at a rate of about 0.5° per day is obtained in the model.

1. Madden, R. A. and Julian, P. R., *J. Atmos. Sci.*, 1971, **28**, 702.
2. Krishnamurti, T. N. and Subrahmanyam, D., *J. Atmos. Sci.*, 1982, **39**, 2088.
3. Krishnamurti, T. N., Jayakumar, P. K., Sheng, J., Surgi, N. and Kumar, A., *J. Atmos. Sci.*, 1985, **42**, 364.
4. Murakami, T. and Nakazawa, T., *J. Atmos. Sci.*, 1985, **42**, 1107.
5. Sikka, D. R. and Gadgil, S., *Mon. Wea. Rev.*, 1980, **108**, 1840.
6. Knutson, T. R., Weickmann, K. M. and Kutzbach, J. E., *Mon. Wea. Rev.*, 1986, **114**, 605.
7. Lau, K. M. and Chan, P. H., *Mon. Wea. Rev.*, 1986, **114**, 1354.
8. Yasunari, T., *J. Meteor. Soc. Jpn.*, 1979, **57**, 227.
9. Yasunari, T., *J. Meteor. Soc. Jpn.*, 1980, **58**, 225.
10. Lau, N. C. and Lau, K. M., *J. Atmos. Sci.*, 1986, **43**, 2023.
11. Kasture, S. V. and Keshavamurty, R. N., *Proc. Indian Acad. Sci. (Earth Planet Sci.)*, 1987, **96**, 49.
12. Webster, P. J. and Chou, L. C., *J. Atmos. Sci.*, 1980, **37**, 368.
13. Webster, P. J., *J. Atmos. Sci.*, 1983, **40**, 2110.
14. Goswami, B. N. and Shukla, J., *J. Atmos. Sci.*, 1984, **41**, 20.
15. Keshavamurty, R. N., Kasture, S. V. and Krishnakumar, V., *Beitr. Phys. Atmos.*, 1986, **49**, 443.
16. Keshavamurty, R. N., Krishnakumar, V. and Kasture, S. V., *Proc. Indian Acad. Sci. (Earth Planet Sci.)*, 1988, **97**, 127.
17. Charney, J. G. and Eliassen, A., *J. Atmos. Sci.*, 1964, **21**, 68.
18. Gadgil, S., Hari Om Ashram Prerit Vikram Sarabhai Award Lectures, 1990, p. 45–58.
19. Bourke, W., *Mon. Wea. Rev.*, 1974, **102**, 687.
20. Bourke, W., McAvaney, B., Puri, K. and Thurling, R., *Methods Computat. Phys.*, 1977, **17**, 267.

Received 16 January 1992; revised accepted 16 March 1992